Convective heat transfer predictions in an axisymmetric jet impinging onto a flat plate using an improved k-ω model

Kubacki S., Dick E.

In: Journal of Computational and Applied Mathematics, 234, 2327-2335, 2010

Convective heat transfer predictions in an axisymmetric jet impinging onto a flat plate using an improved k-ω model

Slawomir Kubacki[a,b,*,1], Erik Dick[a,**,1]

[a] *Department of Flow, Heat and Combustion Mechanics, Ghent University St.-Pietersnieuwstraat 41, B-9000 Ghent, Belgium*

[b] *Institute of Thermal Machinery, Czestochowa University of Technology, Al. Armii Krajowej 21, 42-200 Czestochowa, Poland*

Abstract

The paper discusses the convective heat transfer prediction in turbulent axisymmetric jets impinging onto a flat plate using the k-ω model of Wilcox (2006). Improvements to the heat transfer predictions are obtained in flow regions characterized by large level of strain using an impingement invariant proposed by Manceau (2003). The Manceau term is carefully introduced in order to leave the k-ω model predictions unmodified for reference flows. This is obtained using a blending function of Menter (1994). As an alternative, a modification based on the von Karman length scale is also discussed. Both modifications do not lead to stability problems in flow regions characterized by large levels of strain, preserving the robustness of the k-ω model. Improvements have been obtained for convective heat transfer prediction in stagnation flow regions of axisymmetric jets impinging onto a flat plate with nozzle-plate distances $H/D = 2, 6, 10$ and Reynolds numbers $Re = 23000, 70000$.

Key words: turbulence modelling, impinging jet, convective heat transfer

1. Introduction

Impinging jets are commonly used in industrial and laboratory applications due to high heat transfer coefficients which can be achieved in stagnation flow regions. In industry, impinging jets are frequently applied in processes such as cooling of turbine blades or tempering of glass. Hollworth and Durbin [11] investigated the performance of impinging jets in cooling of electronics. Roy et al. [21] studied air jets impinging on the glass windshield of a vehicle, both experimentally and numerically. In the study of anodizing processes, the wall–jet electrode reactor is quite often employed (with the electrolyte impinging perpendicularly to the electrode). With this configuration a non-uniform heat transfer can be achieved over the electrode, which impacts the local anodic film thickness [6].

*Corresponding author

**Principal corresponding author

Email addresses: Slawomir.Kubacki@UGent.be (Slawomir Kubacki), Erik.Dick@UGent.be (Erik Dick)

[1] Authors acknowledge the support from the research project *Novel multiscale approach to transport phenomena in electrochemical processes* (IWT, contract: MuTEch SBO 040092)

The impinging jet flow is a challenging test case for RANS models. Therefore it is frequently used for their validation. In the present work, the experimental data of Cooper et al. [5] are taken in order to compare the measured and predicted mean and fluctuating velocity profiles. The predicted Nusselt number profiles are compared to experimental data of Baughn and Shimizu [2], Baughn et al. [1], Yan et al. [25] and Lytle and Webb [15]. The k-ω model of Wilcox is employed combined with modifications meant to improve the heat transfer prediction in stagnation flow regions.

Among many eddy-viscosity models, the k-ω model of Wilcox has received great interest because of its usefulness in resolving turbulent flows near walls without requirement of wall damping functions. The reason for this favorable behavior is that 'extra dissipation' is produced near walls compared to the standard k-ϵ model as a result of the so called cross-diffusion term [9]. The cross-diffusion term appears by writing the k-ω model in the k-ϵ formulation. As mentioned by Durbin and Pettersson Reif [9], the near wall behavior of the k-ϵ model is not correct. This is due to insufficient suppression of turbulent mixing by the standard k-ϵ model in wall proximity. In order to avoid this shortcoming near-wall damping functions are introduced. This is in contrast to the k-ω model where an addition of damping functions is not necessary. As stressed by Menter [17] and Pope [20], the k-ω model is superior compared to the k-ϵ model in treatment of the viscous near-wall region as well as in accounting for the effect of an adverse pressure gradient. Although, this inherent property of the k-ω model poses advantages in resolving attached boundary layer flows and mildly separated flows, the accuracy of the earlier versions of the k-ω model was flawed by their sensitivity to the boundary conditions for the ω variable at the far-field boundaries, leading to ambiguous results in prediction of free shear flows [18]. Menter [17, 18] succeeded in resolving the freestream dependency of the k-ω model by blending the standard k-ω model with the standard k-ϵ model (transformed to the k-ω formulation). In [17] a blending function has been applied in order to recover the standard k-ω model close to the walls and switch gradually to the k-ϵ model in the outer part of the boundary layer. As shown by Wilcox [22, 24], a similar effect can be obtained by introducing the cross-diffusion term away from walls and simply switching the cross-diffusion term off when it becomes negative (close to walls). Such a approach has been considered by Kok [14] in the construction of his TNT model. Bredberg et al. [4] introduced the cross-diffusion term in the $\omega-$ equation in such way that it is also active close to walls. As a result, their modified k-ω model is similar to the k-ϵ model (written in the k-ω formulation). A damping function is introduced in the definition of the turbulent viscosity which is similar to what is typically done in k-ϵ models.

In addition to inclusion of a cross-diffusion term in the ω-equation, a stress limiter is applied in the new k-ω model in order to reduce overprediction of the turbulent stress in flow regions characterized by large rates of strain, as in stagnation flow regions [24]. A Similar stress limiter has been previously implemented in the SST model of Menter [17, 18]. Also Durbin [8] derived a stress limiter by a bound on the turbulent time scale from 'realizability constraints'. Heat transfer results of axisymmetric turbulent impinging jet flow with the $v^2 - f$ model of Durbin have been presented in [3].

The objective of the present work is to improve stagnation point heat transfer predictions with a minimum amount of complexity added to the underlying turbulence model. In the present paper, the discussion of the modifications leading to improved convective heat transfer predictions is limited to axisymmetric jets impinging onto a flat plate. The discussion of plane impinging jets is left for future work. A first modification is based on the impingement term of Manceau [16]. The other variant is based on adding a length-scale correction as proposed by Wilcox [24]. In the first modification, only one free coefficient has been introduced (tuned for one of the considered

test cases) and a blending function of Menter has been applied. The other modification involves the von Karman length scale, namely $l_\mu = (\beta^\star)^{-3/4}\kappa y = 2.5y$ [20] (where $\beta^\star = 0.09$, $\kappa = 0.41$ is the von Karman constant and y denotes the distance normal to the wall) in order to correct the turbulent length scale in the near-wall region. The proposed modification based on inclusion of the impingement term has been designed such that results of simulations of free shear flows, channel and pipe flows and the flow over a backward facing step are not changed compared to the original k-ω model results. This is crucial since the model coefficients and the constants in the auxiliary relations have been calibrated for these flows. The modification based on the von Karman length scale can only be used in a limited number of flows such as axisymmetric impinging jets, since some results of reference flows for turbulence models are changed by adding this modification. The two studied variants lead to improvement of the predictions of the heat transfer in the impingement zone. The effect is less away from the core of the impingement zone.

2. Mathematical formulation

2.1. Mean momentum, energy and turbulence model equations

For an incompressible fluid, the Reynolds-averaged continuity, momentum and energy equations can be written as

$$\frac{\partial U_i}{\partial x_i} = 0 \tag{1}$$

$$\frac{\partial(\rho U_i)}{\partial t} + U_j\frac{\partial(\rho U_i)}{\partial x_j} = -\frac{\partial P}{\partial x_i} + \frac{\partial}{\partial x_j}\left(2\mu S_{ij} - \rho\overline{u_i' u_j'}\right) \tag{2}$$

$$\frac{\partial(\rho T)}{\partial t} + U_i\frac{\partial(\rho T)}{\partial x_i} = \frac{\partial}{\partial x_i}\left(\frac{\lambda}{c_p}\frac{\partial T}{\partial x_i} - \rho\overline{u_i'\vartheta'}\right) \tag{3}$$

where ρ is the fluid density, μ is the molecular viscosity, P is the mean pressure, T is the mean temperature, λ is the thermal conductivity, c_p is the specific heat at constant pressure. The vector and tensor components are: U_j of the mean velocity vector, S_{ij} of the rate of strain tensor, $-\rho\overline{u_i' u_j'} = \tau_{ij}$ of the Reynolds stress tensor and $-\rho\overline{u_i'\vartheta'}$ of the turbulent heat flux.

The Boussinesq relation is assumed between the Reynolds stress tensor and the rate of strain tensor

$$-\rho\overline{u_i' u_j'} = \tau_{ij} = 2\rho\nu_t S_{ij} - \frac{2}{3}\rho k\delta_{ij} \tag{4}$$

where the turbulent viscosity is determined by [24]

$$\nu_t = \frac{k}{\tilde{\omega}}, \quad \tilde{\omega} = \max\left\{\omega, C_{lim}\sqrt{2S_{ij}S_{ij}/\beta^*}\right\} \tag{5}$$

The turbulent kinetic energy k and the specific dissipation rate ω in Eq. (5) are determined by solution of the following transport equations

$$\frac{D(\rho k)}{Dt} = \tau_{ij}\frac{\partial U_i}{\partial x_j} - \beta^*\rho k\omega + \frac{\partial}{\partial x_j}\left[\left(\mu + \sigma^*\rho\frac{k}{\omega}\right)\frac{\partial k}{\partial x_j}\right] \tag{6}$$

$$\frac{D(\rho\omega)}{Dt} = \alpha\frac{\omega}{k}\tau_{ij}\frac{\partial U_i}{\partial x_j} - \beta\rho\omega^2 + \rho\frac{\sigma_d}{\omega}\frac{\partial k}{\partial x_j}\frac{\partial\omega}{\partial x_j} + \frac{\partial}{\partial x_j}\left[\left(\mu + \sigma\rho\frac{k}{\omega}\right)\frac{\partial\omega}{\partial x_j}\right] \tag{7}$$

where $D(\cdot)/Dt = \partial(\cdot)/\partial t + U_j \partial(\cdot)/\partial x_j$ denotes the Lagrangian derivative. Notice that $\omega = \epsilon/(\beta^* k)$ can be seen as the reciprocal of the turbulent time scale at which dissipation of turbulent kinetic energy takes place [24].

The model coefficients are

$$\alpha = 0.52, \quad \beta = \beta_0 f_\beta, \quad \beta^* = 0.09, \quad \sigma = 0.5, \quad \sigma^* = 0.6, \quad \sigma_{d0} = 0.125, \quad C_{lim} = 7/8 \tag{8}$$

$$\beta_0 = 0.0708, \quad f_\beta = \frac{1 + 85\chi_\omega}{1 + 100\chi_\omega}, \quad \chi_\omega \equiv \left| \frac{\Omega_{ij}\Omega_{ij}S_{ij}}{(\beta^*\omega)^3} \right| \tag{9}$$

where

$$\sigma_d = \begin{cases} 0 & \text{for} \quad \frac{\partial k}{\partial x_j}\frac{\partial \omega}{\partial x_j} \leq 0 \\ \sigma_{d0} & \text{for} \quad \frac{\partial k}{\partial x_j}\frac{\partial \omega}{\partial x_j} > 0 \end{cases} \tag{10}$$

and Ω_{ij} and S_{ij} are defined by

$$\Omega_{ij} = \frac{1}{2}\left(\frac{\partial U_i}{\partial x_j} - \frac{\partial U_j}{\partial x_i} \right), \quad S_{ij} = \frac{1}{2}\left(\frac{\partial U_i}{\partial x_j} + \frac{\partial U_j}{\partial x_i} \right). \tag{11}$$

One should note that a stress limiter is introduced in Eq. (5) and that the sensitivity of the original k-ω model to the free-stream values is limited by addition of the cross-diffusion term in the ω-equation (third term on the right hand side of Eq. (7)). The cross-diffusion term is only active away from walls (where the term $\partial k/\partial x_j \partial \omega/\partial x_j$ takes positive values, see Eq. 10) while in the near wall region the unmodified k-ω model is used (negative values of $\partial k/\partial x_j \partial \omega/\partial x_j$).

The turbulent heat flux in Eq. (3) is modeled assuming the gradient-diffusion hypothesis

$$\rho \overline{u_i' \vartheta'} = -\frac{\mu_t}{Pr_t}\frac{\partial T}{\partial x_i} \tag{12}$$

where $Pr_t = 0.85$.

At no-slip walls, the following boundary conditions have been applied for k and ω [18]

$$k = 0, \quad \omega = 10\frac{6\nu}{\beta_0(\Delta y)^2} \tag{13}$$

where ν is the kinematic viscosity and Δy is the distance of the first point to the wall.

2.2. Proposed modifications

Although the stress limiter introduced in the definition of the turbulent viscosity (Eq. 5) reduces the spontaneous overproduction of turbulent kinetic energy in stagnation flow regions, in most applications some overproduction remains. Two remedies are proposed here in order to correct the k-ω model predictions in stagnation flow regions. The first modification is based on introducing an impingement function in Eq. (5):

$$\nu_t = \frac{k}{\tilde{\omega}}, \quad \tilde{\omega} = \max\left\{ \omega, C_{lim} F_{imp} \sqrt{\frac{2S_{ij}S_{ij}}{\beta^*}} \right\} \tag{14}$$

The impingement function F_{imp} is defined by

$$F_{imp} = 1 + A_{imp} F_1 P_{norm}, \tag{15}$$

$$P_{norm} = \frac{3}{2}\frac{[\min(P,0)]^2}{\eta^2}, \quad P = \{\mathbf{SM}\}, \quad \eta = \sqrt{\{\mathbf{S}^2\}}, \tag{16}$$

where $\{\cdot\}$ denotes the trace of the tensor. $\mathbf{S}$ is the rate of strain tensor and the components of the tensor $\mathbf{M}$ are $M_{ij} = n_i n_j - 1/3\delta_{ij}$, where n_i is the i-th component of the unit vector normal to the wall. This unit vector also has to be defined in the interior of the flow. A limiter of this type, as first suggested by Manceau [16] for an algebraic stress model, was also found to be very efficient for the k-ϵ model by Merci et al. [19].

The value of the constant A_{imp} in Eq. (15) was set to $A_{imp} = 2.0$ by tuning it for one of the test cases in order to obtain good agreement with the experimental value of the Nusselt number in the stagnation flow region. F_1 is the blending function proposed by Menter [18].

The value of the Manceau term P^2/η^2 [16] (Eq. 16) is equal to $2/3$ in axisymmetric impingement flow regions, approximately equal to $1/2$ for impinging two-dimensional flows and it is zero for boundary layer and channel flows, but it is not guaranteed that the Manceau term will be exactly zero in other flows (e.g. separated shear layer or free shear flows). The Manceau term P^2/η^2 is normalized (multiplying it by the factor $3/2$ in Eq. (16)) in order to impose $P_{norm} = 1$ in axisymmetric impingement flow regions. Since the proposed modification should not change the k-ω model predictions for flows involving separation and reattachment of a boundary layer as well as for free shear flows, the term P_{norm} in Eq. (15) is multiplied by Menter's F_1 function in order to ensure that the limiter is only active close to the wall.

As a second modification, a correction to the length scale is studied as proposed by Wilcox [24] defining the turbulent viscosity by

$$\nu_t = \frac{\beta^* \sqrt{k} l_t}{\max\left[1, \left(C_{lim}\sqrt{\frac{2S_{ij}S_{ij}}{\beta^*}}\right)/\omega\right]} \tag{17}$$

where l_t in Eq. (17) is the turbulent length scale which is defined by

$$l_t = \min\left(l_\mu, \frac{\sqrt{k}}{\beta^*\omega}\right), \quad l_\mu = 2.5y \tag{18}$$

where y is the normal distance to the wall. Note that Eq. (17) reduces to Eq. (5) if $l_t = \sqrt{k}/(\beta^*\omega)$ in Eq. (18). In stagnation flow regions, the turbulent length scale is overpredicted by the k-ω model, so that Eq. (18) limits the turbulent viscosity.

3. Results

Results are presented for simulation of an axisymmetric jet impinging onto a flat plate. In order to perform a critical evaluation of the proposed modifications, the following flows have been also analyzed: plane and axisymmetric jet flows, pipe and channel flows and flow over a backward facing step. The modification based on the impingement function does not change the k-ω results for free shear flows, pipe and 2-D channel flows. We analyze here the influence of the modifications on the predicted mean velocity profile for free axisymmetric jet simulation as well as on the skin friction coefficient for the flow over a backward facing step.

For the two-dimensional and axisymmetric jet flow simulations (free/impinging onto a flat plate) fully developed profiles were specified at the inlet to the computational domain (separately computed assuming periodic boundary conditions). The inlet boundary was specified one nozzle

width/diameter upstream of the jet exit. For simulation of the fully developed turbulent pipe-flow and the 2D channel flow the Reynolds numbers were specified at $Re_D = 40000$, $Re_H = 13750$, respectively (the Reynolds number is based on the average velocity and on pipe diameter or channel height). For the flow past a backward-facing step the inlet boundary conditions have been obtained from a precursor simulation of a developing 2D channel flow. The mean velocity and the turbulent quantities (k and ω) have been taken from the section where the predicted momentum thickness θ was equal to the experimentally measured value $Re_\theta = 5000$ [12].

All computations have been preformed with the Fluent code ver. 6.2.16. The second order upwind scheme was applied for approximation of the convective terms in the momentum, energy, k- and ω-equations. The SIMPLE algorithm was used for pressure-velocity coupling. In all simulations structured grids have been applied. y^+ was less than 3 at all walls while for simulation of the axisymmetric jet flows impinging onto a flat plate $y^+ < 0.5$ at the impingement plate. The computations have been performed on different grids in order to ensure that grid independent solutions have been obtained.

3.1. Impinging jets

Fig. 1 shows contour plots of turbulent to molecular viscosity ratio close to the impingement point region using (a) the k-ω model, (b) the k-ω model together with the impingement function (Eq. 14) and (c) the k-ω model together with the length scale correction (Eq. 17) for $H/D = 2$ and $Re = 23000$. As mentioned previously, the stress limiter which is already present in the k-ω model limits overprediction of the turbulent length scale in the stagnation flow region (Fig. 1a) which can be recognized by a relatively low level of $\nu_t/\nu \approx$ 10-20. As shown in Fig. 1b the impingement function provides higher damping of the turbulent kinetic energy than using the pure k-ω model. Using the length-scale correction (Fig. 1c) results in reduced values of ν_t/ν at $X/R > 1.8$. It should be remarked that both proposed modifications do not change the pure k-ω results in the flow regions away from the impingement zone.

Fig. 2 shows the predicted and measured velocity magnitudes and fluctuating velocity components (parallel and normal to the wall) at different radial positions from the symmetry axis (along lines perpendicular to the impingement plate) for the nozzle-plate distance $H/D = 2$ and $Re = 23000$. Since an isotropic turbulence model is applied here, the fluctuating velocity components have been computed by $u' = v' = \sqrt{2/3k}$. The data are normalized by the bulk velocity U_b at the jet exit and they are plotted as a function of the dimensionless distance from the wall $(H - x)/D$, were H is the nozzle-plate distance and D is the nozzle diameter. The predicted mean and fluctuating velocity profiles are compared to the experimental data of Cooper et al. [5]. The solid lines represent the k-ω results, the dashed lines represent the results obtained using the k-ω model together with the modification based on the Manceau term (Eq. 14) and the dashed-dotted lines represent the results obtained using the k-ω model together with the modification based on the von Karman length scale (Eq. 17). Both mean and fluctuating velocity profiles are well predicted close to the impingement point region ($R/D = 0.5$) using the k-ω model (Figs. 2a,c and e). This is a consequence of limiting the turbulent stress in the stagnation flow region by the stress limiter. However, there is a slight overestimation of the turbulent kinetic energy near the wall. This overestimation is reduced by the proposed modifications. At the distance $R/D = 1$ (Figs. 2b,d and f) the predicted fluctuating velocity components fall between the experimentally measured values of u'/U_b and v'/U_b for $(H - x)/D < 0.2$. Again, the slight overestimation of the turbulent kinetic energy is reduced by the proposed modifications. Good agreement between predictions and measurements has been also obtained at larger distances from the symmetry

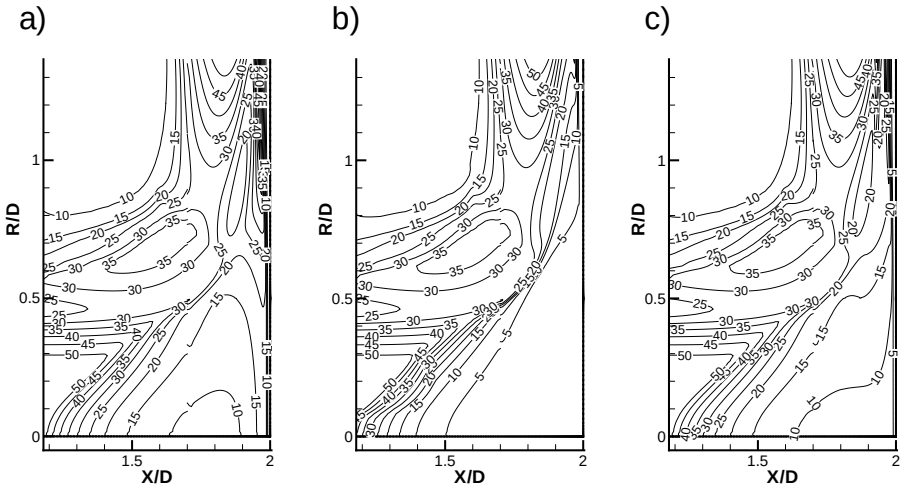

Figure 1: Contour plots of turbulent to molecular viscosity ratio close to the impingement point region using (a) k-ω model (b) k-ω model together with the impingement function and (c) k-ω model together with the length scale correction for $H/D = 2$ and $Re = 23000$.

axis and in the other test cases analyzed (assuming different values of the Reynolds number $Re = 23000, 70000$ and different nozzle-plate distances $H/D = 2, 6$).

One may ask whether reducing the turbulent kinetic energy in the near-wall region (say at $(H - x)/D < 0.1$, Fig. 2c-f) can be considered as a real improvement to the k-ω model. As mentioned by Durbin [7] the wall normal fluctuating velocity components are more relevant to the heat transfer at the solid walls. Therefore it is very important to mimic this behavior in order to improve the heat transfer predictions in the stagnation flow region.

Fig. 3a shows the predicted heat transfer rates along the impingement plate obtained using the k-ω model (solid lines), applying the k-ω model together with the proposed modification based on impingement function (dashed lines) and applying the k-ω model together with the proposed modification based on von Karman length scale (dashed-dotted lines) for $H/D = 2, Re = 23000$. The dashed double-dotted line ($D_t = 0$) depicts the Nusselt number obtained for the turbulent flow simulation using the k-ω model and setting to zero the turbulent diffusivity in the energy equation. The predicted heat transfer rates are compared to the experimental data of Baughn and Shimizu [2], Baughn et al. [1], Yan et al. [25] and Lytle and Webb [15]. Application of the impingement detector (Eq. 14) damps the turbulent kinetic energy in the stagnation flow region giving better correspondence between predictions and experiments than using the standard k-ω model. The length-scale correction based on the von Karman length scale (Eq. 17) gives almost the same value of stagnation point Nusselt number as using the impingement detector. Both modifications are inactive very close to the wall and the predicted heat transfer rates are slightly higher than the heat transfer rates determined by setting to zero the turbulent diffusivity in the energy equation. This is due to the fact that the Manceau term (P^2/η^2) is zero inside most of the boundary layer. Similarly, the length-scale correction is inactive close to the wall due to the large value of ω in Eq. (13). Away from the wall, the Manceau term becomes active ($F_{imp} > 1$ in Eq. 15) reducing anomalous overprediction of turbulent kinetic energy in the stagnation flow regions. Similarly, for the second proposed modification, the length scale l_μ becomes smaller than

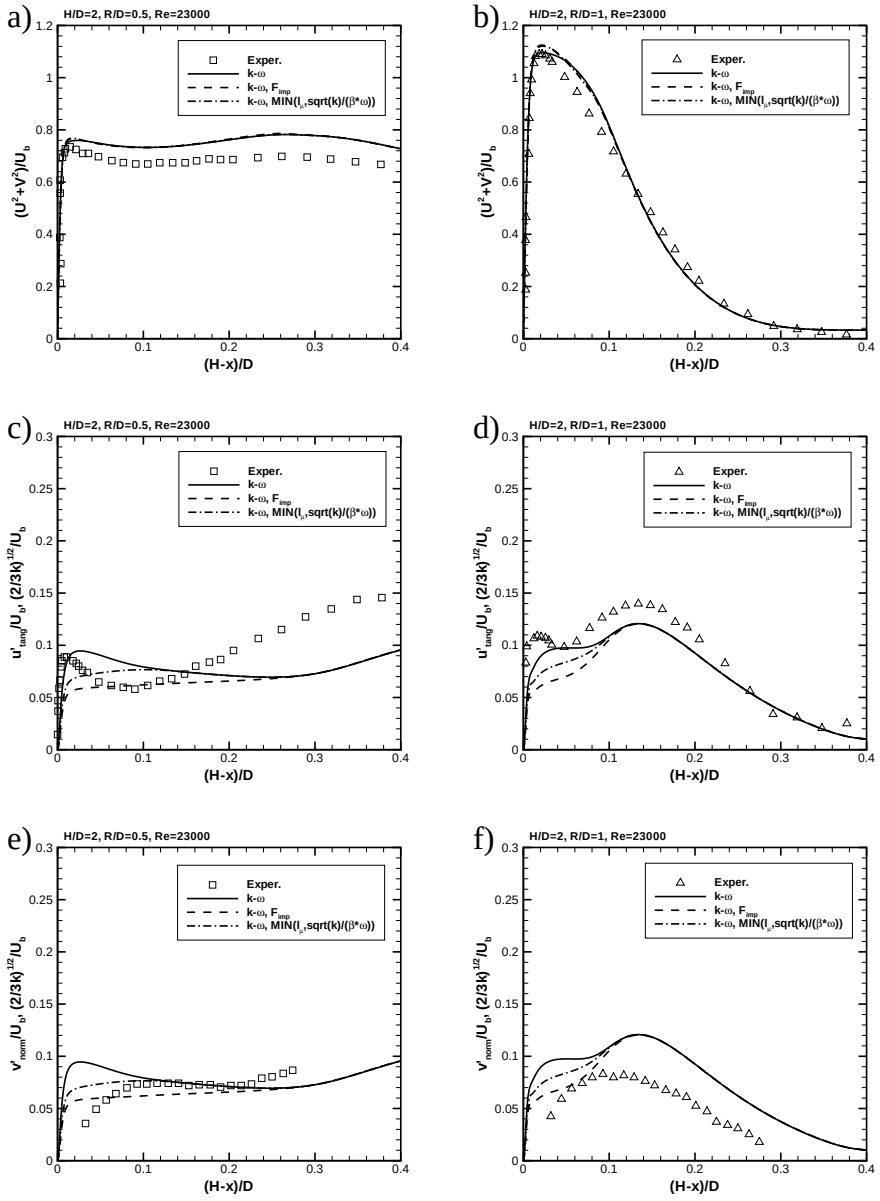

Figure 2: Profiles of velocity magnitude (top) and fluctuating velocity components (parallel to the wall -middle, normal to the wall -bottom) at the distance $R/D = 0.5$ (a,c and e), and $R/D = 1$ (b,d and f) from the symmetry axis for $H/D = 2, Re = 23000$.

$\sqrt{k}/(\beta^*\omega)$ suppressing the turbulent kinetic energy production in the stagnation flow region. At larger distances from the wall the value of l_μ (Eq. 18) becomes large and the turbulent viscosity is again provided by the turbulence model. The asymptotic behavior of the predicted profiles of the Nusselt number at larger distances from the symmetry axis (R/D >3, Fig. 3a) is not well reproduced by the k-ω model. The same conclusion can be drawn from work of Jarmaillo et al. [13] where a previous version of the k-ω model [23] has been applied for simulation of axisymmetric and plane impinging jets. For cases with moderate Reynolds number (Re = 23000), the k-ω model has a tendency to underpredict turbulent kinetic energy in the wall jet region at larger distances from the symmetry axis. As shown in Fig 3b ($H/D = 2, Re = 70000$) the stagnation Nusselt number is better predicted using the impingement detector than applying the length scale correction. The secondary peak in the Nusselt number distribution is well recovered using both modifications. The dip in the Nusselt number distribution at $R/D = 1$ is not well reproduced. Fig. 3c shows the heat transfer rates predicted for $H/D = 6, Re = 23000$. Note the quite large difference in the measured heat transfer rates. For this case, the stagnation point Nusselt number is slightly underpredicted using the impingement detector and it is well predicted using the length scale correction. For higher Reynolds number flow ($H/D = 6, Re = 70000$), shown in Fig 3d, the stagnation point Nusselt number is again well predicted with both modifications but the predicted heat transfer rates are still too high at $1 < R/D < 3$. An improvement in the prediction of the stagnation point Nusselt number is also obtained for the nozzle-plate distance $H/D = 10$ and $Re = 23000$ (Fig. 3e).

3.2. Free jet flow and flow over a backward-facing step

Fig. 4a, shows the profile of the mean velocity (normalized by velocity at the jet axis) along y/x (where y- and x- denote the radial and axial coordinates, respectively) at distance $x/D = 5$ from the jet exit for simulation of a free axisymmetric jet flow using the k-ω model and applying the modifications. The results are not modified with the added modifications to the k-ω model.

Fig. 4b, shows the predicted skin friction coefficient c_f using the k-ω model and applying the modifications for a backward facing step. The results of the simulation are compared with the experimental data of Driver and Seegmiller [10]. The k-ω model predicts the reattachment at 6.88 step heights downstream of the step. The same result is obtained with the k-ω model and the modification based on the impingement detector. This is within 10% of the measured value $6.26H$ (where H is the step height). Since the Manceau term in Eq. (15) is zero in simple shear flows, the limiter is only active right after the corner. Menter's F_1 function in Eq. (15) bounds the limiter to be active close to the wall and the function F_{imp} goes gradually to unity in the separated flow region. Application of the length-scale correction based on the von Karman length scale gives a reattachment at $7.2H$ which is 15% larger than the measured value. This cannot be accepted since the predicted length of the separation bubble becomes too large compared to the value experimentally measured and predicted by the k-ω model. Furthermore, the predicted values of c_f are also modified downstream of the step.

4. Summary

Improved stagnation point heat transfer predictions have been obtained for simulation of axisymmetric jet flows impinging onto a flat plate with modifications of the k-ω model based on an impingement detector and on a length scale correction. Verification of the added modifications has been demonstrated for free shear flow and the flow over a backward facing step. The analysis

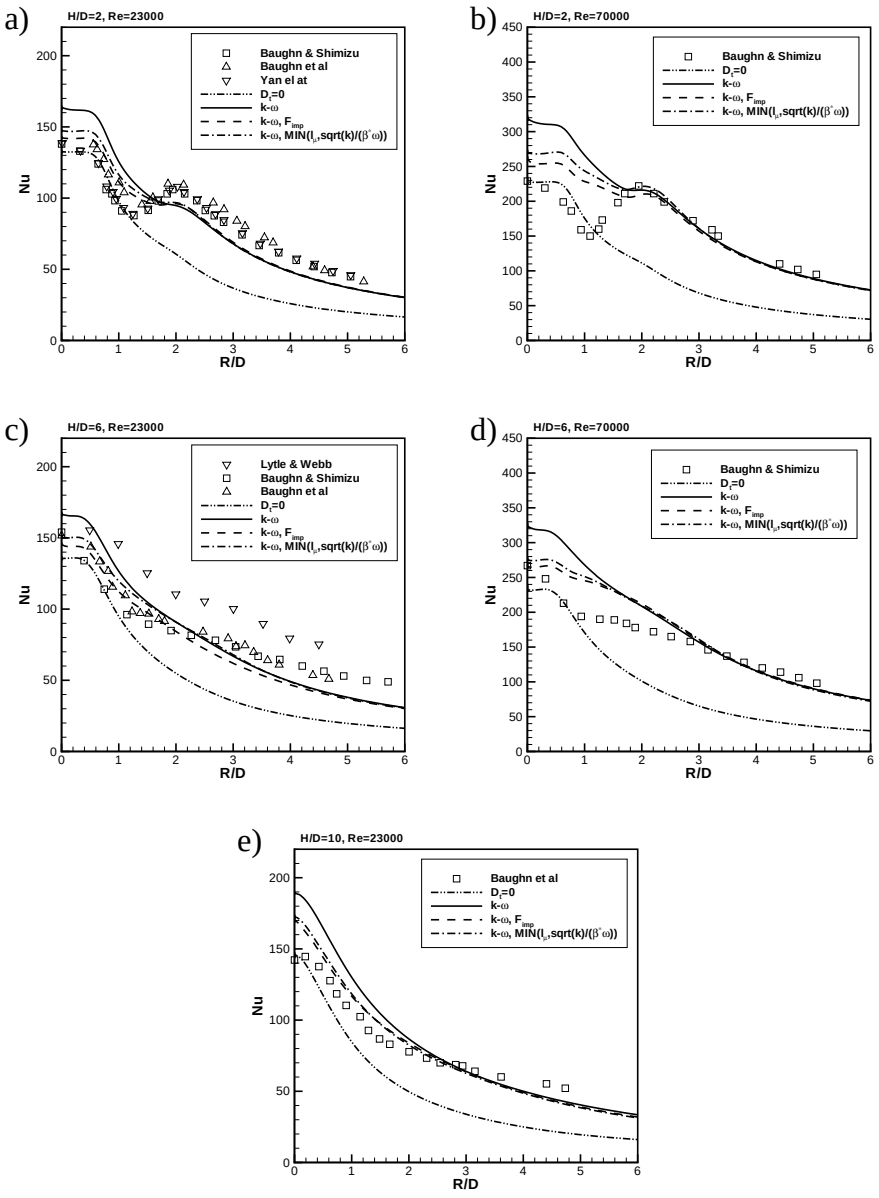

Figure 3: Nusselt number distribution along a flat plate for a). $H/D = 2, Re = 23000$, b). $H/D = 2, Re = 70000$, c). $H/D = 6, Re = 23000$, d). $H/D = 6, Re = 70000$, e). $H/D = 10, Re = 23000$. $D_t = 0$ denotes the Nusselt number obtained for the turbulent flow simulation using the k-ω model but setting to zero the turbulent diffusivity in the energy equation.

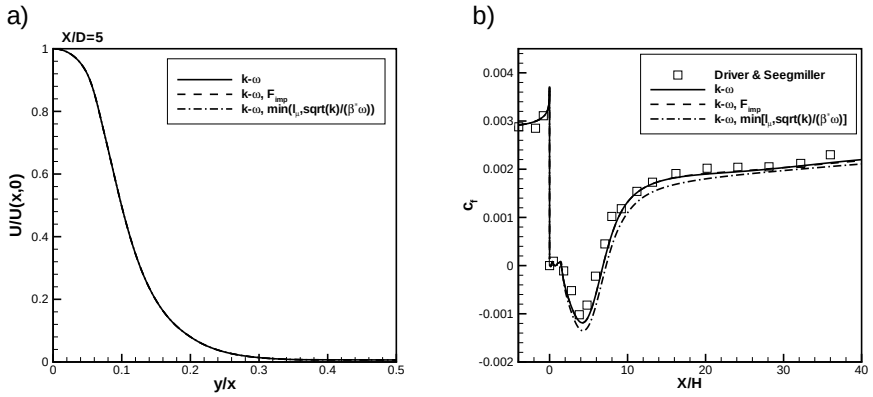

Figure 4: (a) Predicted mean velocity profiles for simulation of the axisymmetric jet flow at distance $X/D = 5$ from the jet exit (b) computed and measured skin friction coefficient for the flow over a backward facing step, $Re_\theta = 5000$.

showed that only the impingement detector based on the invariant of Manceau can be considered as a more general formulation in order to improve heat transfer predictions in stagnation flow regions, so this modification is recommended. The length scale correction based on the von Karman length can only be used in a limited number of flows such as axisymmetric jet flows impinging onto a flat plate, so it is not recommended.

References

[1] J.W. Baughn, A.E. Hechanova and X. Yan, An experimental study of entrainment effects on the heat transfer from a flat surface to a heated circular impinging jet, *J. of Heat Transfer*, **113**(4) (1991) 1023-1025.

[2] J.W. Baughn and S. Shimizu, Heat transfer measurements from a surface with uniform heat flux and an impinging jet, *J. of Heat Transfer* **111**(4) (1989) 1096-1098.

[3] M. Behnia, S. Parneix and P.A. Durbin. Prediction of heat transfer in an axisymmetric jet impinging on a flat plate. *Int. J. Heat Mass Transfer*, **41**(12) (1998) 1845-1855.

[4] J. Bredberg, S-H Peng, L. Davidson, An improved *k-ω* turbulence model applied to recirculating flows, *Int. J. Heat Fluid Flow*, **23** (2002) 731-743.

[5] D. Cooper, D.C. Jackson, B.E. Launder and G.X. Liao, Impinging jet studies for turbulence model assessment-I. Flow-field experiments, *Int. J. Heat Mass Transfer*, **36**(10) (1993) 2675-2684.

[6] I. De Graeve, H. Terryn and G.E. Thompson, Influence of local heat development on film thickness for anodizing aluminum in sulfuric acid, *J. of the Electroch. Soc.*, **150**(4) (2003) 158-165.

[7] P.A. Durbin, Near-wall turbulence closure without damping functions, *Theoretical and Computational Fluid Dynamics*, **3**(1) (1991) 1-9.

[8] P.A. Durbin, On the *k-ϵ* stagnation point anomaly. *Int. J. Heat Fluid Flow*, **17** (1996) 89-90.

[9] P.A. Durbin and B.A. Pettersson Reif, *Statistical theory and modeling for turbulent flows*, John Wiley & Sons, 2001.

[10] D.M. Driver and H.L. Seegmiller, Features of reattaching turbulent shear layer in divergent channel flow, *AIAA Journal*, **23**(1) (1985) 163-171.

[11] B.R. Hollworth, M. Durbin, Impingement cooling of electronics, *J. of Heat Transfer*, **114** (1992) 607-613.

[12] J.E. Jaramillo, C.D. Perez-Segarra, A. Oliva and K. Claramount, Analysis of different RANS models applied to turbulent forced convection. *Int. J. Heat Mass Transfer*, **50**(19-20) (2007) 3749-3766.

[13] J.E. Jaramillo, C.D. Perez-Segarra, I. Rodriguez and A. Oliva, Numerical study of plane and round impinging jets using RANS models, *Numer. Heat Transfer, Part B*, **54** (2008) 213-237.

[14] J.C. Kok, Resolving the dependence on freestream values for the *k-ω* turbulence model, *AIAA Journal*, **38**(7) (2000) 1292-1295.

[15] D. Lytle and B. Webb, Air jet impingement heat transfer at low nozzle-plate spacings, *Int. J. Heat Mass Transfer*, **37**(2) (1994) 1687-1697.

[16] R. Manceau, Accounting for wall-induced Reynolds stress anisotropy in an explicit algebraic stress model, in: N. Kasagi et al.(Ed.), Proc. Third Int. Symp. on Turbulence and Shear Flow Phenomena, Vol. I., Sendai, Japan, 2003.
[17] F.R. Menter, Zonal two equation k-ω turbulence models for aerodynamic flows, *AIAA Paper* 93-2905 (1993).
[18] F.R. Menter, Two-equation eddy-viscosity turbulence models for engineering applications, *AIAA Journal*, **32**(8) (1994) 1598-1605.
[19] B. Merci, K. Van Maele and E. Dick, Impingement heat transfer with a nonlinear first-order $k-\epsilon$ model, *J. Thermophysics and Heat Transfer*, **20**(1) (2005) 144-148.
[20] S.B. Pope, *Turbulent flows*, Cambridge University Press, 2000.
[21] S. Roy, K. Nasr, P.Patel, B. AbdulNour, An experimental and numerical study of heat transfer off an inclined surface subject to an impinging airflow, *Int. J. of Heat and Mass Transfer*, **45** (2002) 1615-1629.
[22] D.C. Wilcox, A two-equation turbulence model for wall-bounded and free-shear flows, *AIAA Paper* 93-2905, 1993.
[23] D.C. Wilcox, *Turbulence Modeling for CFD*, 2nd ed., DCW Industries, Inc. La Canada, California, 1998.
[24] D.C. Wilcox, *Turbulence Modeling for CFD*, 3rd ed., DCW Industries, Inc. La Canada, California, 2006.
[25] X. Yan, J.W. Baughn, M. Mesbah, The effect of Reynolds number on the heat transfer distribution from a flat plate to an impinging jet, *ASME HTD*, **226** (1992) 1-7.